Translational dynamics of ionic liquid imidazolium cations at solid/liquid interface in gel polymer electrolyte

ARTICLE *in* EUROPEAN POLYMER JOURNAL · AUGUST 2015

Impact Factor: 3.01 · DOI: 10.1016/j.eurpolymj.2015.08.001

4 AUTHORS, INCLUDING:

Ewa Andrzejewska

Poznan University of Technology

124 PUBLICATIONS **1,443** CITATIONS

SEE PROFILE

Agata Dembna

Saint-Gobain Abrasives

12 PUBLICATIONS **9** CITATIONS

SEE PROFILE

Jadwiga Tritt-Goc

Institute of Molecular Physics, Polish A…

84 PUBLICATIONS **726** CITATIONS

SEE PROFILE

European Polymer Journal 71 (2015) 210–220

Contents lists available at ScienceDirect

European Polymer Journal

journal homepage: www.elsevier.com/locate/europolj

Translational dynamics of ionic liquid imidazolium cations at solid/liquid interface in gel polymer electrolyte

Adam Rachocki [a,*], Ewa Andrzejewska [b], Agata Dembna [b], Jadwiga Tritt-Goc [a]

[a] Institute of Molecular Physics, Polish Academy of Sciences, M. Smoluchowskiego 17, 60-179 Poznan, Poland
[b] Faculty of Chemical Technology, Poznan University of Technology, Berdychowo 4, 60-965 Poznan, Poland

ARTICLE INFO

Article history:
Received 28 April 2015
Received in revised form 20 July 2015
Accepted 2 August 2015
Available online 3 August 2015

Keywords:
Gel polymer electrolyte
Ionic liquid
Photopolymerization
Translational diffusion
Surface diffusion
Fast field-cycling NMR relaxometry

ABSTRACT

Gel polymer electrolyte (GPE) based on ethoxylated bisphenol A dimethacrylate and 1-butyl-3-methylimidazolium tetrafluoroborate ([BMIm][BF_4]) ionic liquid (IL) at the mass ratio of 20:80 was prepared by *in situ* photopolymerization. The obtained material showed an exceptional behavior: its ionic conductivity was approximately twice higher than that of pure IL (as measured by impedance method). To explain the observed effect the translational diffusion of cations was studied indirectly by means of fast field-cycling (FFC) proton (^{1}H) nuclear magnetic resonance (NMR) relaxometry method. The spin–lattice relaxation times of proton in cations were measured for neat IL and the IL involved in the polymer matrix in the temperature range from 248 to 343 K. The relaxation data obtained for bulk IL were analyzed in terms of both translational self-diffusion (*Torrey's model*) and local molecular reorientations around a long and a short molecular axis of the IL cation (*Woessner's model*). The relaxation of IL confined to polymer matrix revealed a low-frequency dispersion (not observed for bulk liquid) which is the fingerprint of the ionic liquid cations/polymer matrix interactions. Therefore, the low-frequency NMR relaxation data in GPE were analyzed assuming the *reorientation mediated by translational displacements* (RMTD) mechanism. This dynamic process allows to explain a very long correlation time of the order of 10^{-5} s calculated for the cations at the polymer/IL interface and determine their diffusion coefficient. It was found that the latter is unexpectedly higher than that of the self-diffusion constant of cations in pure IL and/or inside pools of IL in the polymer matrix. This finding indicates that in the presence of the GPE matrix new cation-conducting pathways may be created which play an important role in ionic conduction at the microscopic and/or quasi-macroscopic scale.

1. Introduction

Translational dynamics of particles (molecules or ions) has fundamental meaning for all important transport processes occurring in micro-scale in nature and therefore is extensively explored in different molecular systems [1–4]. For ionic liquids (ILs), the translational modes of the molecular dynamics of ions potentially provide the information on interionic interactions or molecular rearrangements reflecting complex diffusion processes associated, among others, directly with ionic conductivity [5–7]. For electrochemical use of ionic liquids, it is particularly important to find correlations between

* Corresponding author.
E-mail address: adam.rachocki@ifmpan.poznan.pl (A. Rachocki).

http://dx.doi.org/10.1016/j.eurpolymj.2015.08.001
0014-3057/

the motions and interactions of IL ions occurring at the molecular level and relate them to the macroscopic scale giving substantial arguments for further development, for instance, of alternative IL-based electrolytes used in electrochemical devices, such as solid-state batteries, capacitors, fuel cells, energy storage, and chemical sensors [8–15].

In situ photopolymerization is especially attractive method of preparation of novel solid polymer electrolytes with ionic conductivity suitable for practical applications (above 1 mS/cm) [16–20]. This technique involves photocuring of a homogeneous mixture composed of a monomer (the polymer matrix precursor) and an IL, and enables preparation of a gel polymer electrolyte (GPE) in a few minutes. It is also important to emphasize that the *in situ* method provides precise control of composition of the resulting GPEs [21,22], as opposed to the socking method, where the amount of liquid electrolyte absorbed by a polymer matrix is difficult to control [23].

Morphology of the IL-containing GPEs can differ, depending on the compatibility of the polymer matrix and the IL used. GPEs can show phase separation, partial phase separation or can be homogeneous. According to our results [24] phase separation plays a crucial role in obtaining of high GPE conductivity since it is necessary to render pathways continuous for ion transport.

In this paper we applied the photopolymerization technique to obtain highly conductive GPE with separated polymer and IL phases. The matrix precursor was bisphenol A ethoxylate (2 EO/phenol) dimethacrylate (bisAEA4) and the IL was 1-butyl-3-methylimidazolium tetrafluoroborate ([BMIm][BF_4]). The obtained heterogeneous material showed exceptional behavior: its ionic conductivity at 25 °C (6.5 mS/cm) was almost twice higher than that of pure IL (3.76 mS/cm). Similar results were obtained by us also for other polymer electrolytes [21,22]. The aim of the present work was to explain the observed enhancement of the ionic conductivity in the context of the ionic diffusion at the *polymer/IL interface* formed on the border of the solid polymer phase and ionic liquid one.

From the ionic conductivity point of view, the transport of both cations and anions across the polymer electrolyte should be considered. Despite the fact that in ideal ILs all ions are fully dissociated, in real liquids they are to some extent aggregated and do not contribute to the overall electric conductivity [25]. Moreover, the differentiation of both cation and anion contributions to the overall ionic conductivity is extremely complicated exclusively on the basis of the quasi-macroscopic measurements applying an electrical stimulus. In this aspect, nuclear magnetic resonance (NMR) method is more sensitive and especially more selective one which allows to determine separately the microscopic ion dynamics. The advantage of this method over other ones is that it can be employed in a number of ways, including spectroscopy, diffusometry or relaxometry, to provide a variety of information, but first of all, it allows selective identification of the dynamic properties of each type of ions if only the anions and cations are differentiated by their own "NMR-active" nuclei [7,26–28]. Using commercially available NMR spectrometers the diffusion measurements are carried out routinely, particularly in liquids and soft matter, by applying the pulsed magnetic field gradient (up to 30–40 T/m) that encodes the spatial information about nuclear spins travelling with molecules [29]. Another gradient NMR method applying static magnetic field gradient (even up to 180 T/m) has considerably expanded the perspectives for the measurements of small self-diffusion coefficients (down to about 10^{-15} m^2/s) in supercooled liquids or molecular crystals, long chain polymer dynamics, restricted diffusion in systems of confined mesoscopic geometries or anomalous diffusion on fractal structures [30]. The pulsed and static field gradient NMR techniques can be classified as direct ones because the diffusion coefficients are determined directly from the NMR signal attenuation, recorded as a function of the magnetic field gradient strength and/or the time at which the diffusion is followed. Recently, the fast field-cycling (FFC) NMR relaxometry technique has been also successfully used for characterization of the translational diffusion, especially in liquid and soft systems [4,26,27,31,32]. This indirect and non-gradient method gives the possibility to determine the diffusion coefficient from measured frequency dependency (dispersion profile) of spin–lattice relaxation time by applying a suitable theoretical model describing the dynamics of the molecules (ions). Contrary to the gradient techniques, the relaxometry method is uniquely sensitive to the NMR signal of the spin nuclei belonging to a low-abundant fraction of molecules as far as their molecular dynamics is significantly differentiated from that of the high abundant one. This is particularly evidenced for liquid molecules adsorbed at pore walls in porous materials where the NMR diffusometry applying pulsed-field gradient (PFG) plays a minor role, whereas the FFC NMR relaxometry allows to follow the diffusion of adsorbed molecules based on specific relaxation mechanisms [33].

In the present study we are particularly interested in the important issue of the molecular diffusion of IL ions in a gel polymer electrolyte. Especially, the ionic diffusion at the polymer/IL interface forming on the border of the solid polymer and ionic liquid phases is carefully examined. The translational diffusion of the ions is studied by means of FFC NMR relaxometry. It should be emphasized that applying the nuclear magnetic resonance relaxometry method and proper theoretical models for the relaxation data we were able to distinguish the translational dynamics of the IL cations within the separated IL phase of GPE and of the cations interacting with the polymer matrix at the polymer/IL interface. It would be expected that the ion diffusion in the polymeric electrolyte should be slowed down as a result of confinement effects of the polymer matrix related to the geometrical restrictions of pores and/or IL-polymer matrix interactions. However, the obtained results have shown that the diffusion coefficient of the confined IL is comparable with that of neat IL. This result indicates that the cavities in the polymer matrix are large enough and do not restrict the translational diffusion of the IL molecules. On the other hand, the diffusion of the IL cations along the polymer matrix "surface" is significantly enhanced and the calculated diffusion constant is higher than that of pure IL.

2. Experimental section

[BMIm][BF_4] of high purity ($\geqslant$99.0%, water content and halide content $\leqslant$ 100 ppm) was purchased from Merck. Before use the ionic liquid was dried by several cycles of vacuum pumping and aeration under dry nitrogen atmosphere. For NMR studies approximately 1 mL of dry IL was sealed in a gas tube. The density of the pure IL was equal to 1.21 g/cm. The calculated number of ^{1}H and ^{19}F spins per unit volume was equal to 4.84×10^{28} and 1.29×10^{28} m^{-3}, respectively.

Bisphenol A ethoxylate (2 EO/phenol) dimethacrylate (bisAEA4, MW $\sim$ 512) was purchased from Sigma-Aldrich and was dried under vacuum at elevated temperature before use.

The GPE was prepared by mixing the bisAEA4 and [BMIm][BF_4] in the 20:80 weight ratio to give the homogeneous solution, in which 1% of 2,2-dimethoxy-2-phenylacetophenone (photoinitiator, Sigma-Aldrich) has been then dissolved. The composition was polymerized in a metal mold under UV-light (Dymax 5000-EC UV Flood Lamp) for 15 min in an argon filled glove box (H_2O content below 0.1% RH). The obtained turbid material was flexible and self-standing. For the NMR investigation a sample in the form of cylinder with a height of about 1.5 cm and diameter of about 8.5 mm composed of few slices of the GPE material was sealed in an NMR glass tube.

The ionic conductivities of the GPE samples were measured by electrochemical impedance spectroscopy using an impedance analyzer (mAutoLab FRA type III electrochemical system, EcoChemie, the Netherlands) [34].

Proton NMR spin–lattice relaxation measurements were performed as a function of the magnetic field strength with the help of a FFC NMR relaxometer (Stelar s.r.l., Mede, Italy), covering the ^{1}H Larmor frequencies from 10 kHz to 30 MHz. The spectrometer operates by switching the magnetic field produced by electric current flowing in a solenoid coil from a polarizing field (B_{POL}), at which an initial equilibrium of a nuclear magnetization is reached, to a field of interest (B_{RELAX}), at which the nuclear spins relax to the new equilibrium state with a characteristic time constant, T_1 (i.e., the spin–lattice or longitudinal relaxation time). After a delay time, τ, the B_{RELAX} field is switched to the acquisition one (B_{ACQ}) at which a free-induction decay (FID) signal is detected after a simple 90° RF pulse. The detected NMR signal is proportional to the magnetization growth at B_{RELAX} field and is recorded as a function of the delay time τ for a number of B_{RELAX} fields. In the present experiments, the 90° RF-pulse was equal to 9.5 μs, the field switching time was 2.5 ms, the B_{POL} and B_{ACQ} fields corresponded to the ^{1}H Larmor frequency of 24 and 16.3 MHz, respectively. For both bulk IL and polymer electrolyte samples, the measurements were carried out at exactly the same temperatures chosen from the range of 248–343 K. The temperature of the samples was controlled to an accuracy better than 0.5 K.

A monoexponential magnetization decay/recovery was observed at each B_{RELAX} field and at all studied temperatures, and thus, the relaxation times T_1 were calculated from the fits of a single exponential function to the experimental data. The number of accumulations was varied at accessible B_{RELAX} fields and it was set in such a way that the uncertainty of the relaxation times T_1 determined from the fits did not exceed 0.5%.

The NMR signal measured comes mainly from the IL protons because the contribution of the polymer matrix protons, which form a rigid matrix in the gel phase with restricted motion, is undetectable under the applied NMR measuring conditions.

3. Results and discussion

The choice of this ionic liquid for the present study was dictated by the fact that a combination of appropriately selected ions allows obtaining selective NMR information on molecular dynamics of cations and anions by probing, respectively, protons (^{1}H) belonging exclusively to [BMIm]$^+$ and independently fluorine atoms (^{19}F) included only in [BF_4]$^-$ ions. The molecular size and shape of both ions are significantly different. The cation consists of a large methylimidazolium "head" and long butyl "tail", whereas the much smaller anion contains only the boron atom in the central position surrounded

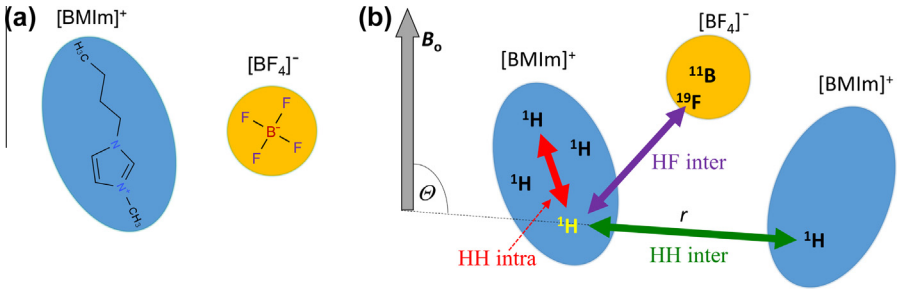

Fig. 1. The chemical structure of 1-butyl-3-methylimidazolium tetrafluoroborate ions (a) and the dipole–dipole interactions crucial for the ^{1}H NMR spin–lattice relaxation (b). The cations are represented by the ellipses and the anion by the circle. HH and HF symbols denote the homo-^{1}H–^{1}H and heteronuclear ^{1}H–^{19}F couplings, respectively. *Intra* and *inter* abbreviations stand for intra- and intermolecular interactions, respectively. $\boldsymbol{B_o}$ is the magnetic field direction, $\boldsymbol{r}$ is the inter-spin vector, and θ is the angle between $\boldsymbol{B_o}$ and $\boldsymbol{r}$.

by four fluorine atoms. Roughly estimated molecular lengths of $[BF_4]^-$ and $[BMIm]^+$ are 4 and 10 Å, respectively [35]. Schematically, the chemical structure of the both ions is presented in Fig. 1a.

Generally, the presence of oscillating electromagnetic fields in the vicinity of a nuclear spin is crucial for NMR transitions between the spin energy levels. Local magnetic fields are generated in several ways and their fluctuations are caused by random motions of molecules. Although Coulombic interactions (along with, van der Waals, hydrogen-bonding, and π–π interactions) are predominant between IL ions [25], from the viewpoint of the nuclear magnetic relaxation theory in liquids, the direct dipole–dipole (dipolar) interactions between nearby nuclear spins, appearing when the magnetic field of one spin affects the local magnetic field of another one, are the most important ones responsible for the relaxation processes [36].

3.1. ^{1}H NMR relaxation in bulk IL

As sketched in Fig. 1b, for IL under investigation, the dipolar interactions can be divided into the intra- and intermolecular ones, if the two spins concerned belong to the same or neighboring ions, respectively. The latter interaction are modulated in time due to the translational dynamics of the ions that changes both the distance, r, between two coupled spins and the angle, θ, between the vector $\boldsymbol{r}$ and an external magnetic field direction $\boldsymbol{B_0}$. The intramolecular dipolar couplings are mainly modulated by the relatively fast rotational dynamics of the ions characterized by the rotational correlation time, τ_{rot}, and effectively influence the spin–lattice relaxation in high magnetic fields.

As was reported recently for ionic liquids containing [BMIm] cations, homonuclear (^{1}H–^{1}H) intermolecular (interionic) couplings were considered as a major source of the proton spin–lattice relaxation measured in low magnetic fields [26,27]. Other couplings between spins of the nuclear spin number 1/2, i.e., ^{1}H–^{19}F intermolecular ones (see Fig. 1b), can be neglected, in the first approximation because approximately four times less fluorine spins then protons are located in the same unit volume of $[BMIm][BF_4]$ IL. The interactions of other "NMR-active" nuclei, such as ^{1}H–^{11}B (3/2 spin), ^{1}H–^{14}N (1 spin) or ^{1}H–^{13}C (1/2 spin), also bring a negligible contribution to the proton relaxation in the studied IL due to relatively low concentrations of the spins or small gyromagnetic factors.

With respect to the above simplification only the proton dipole–dipole interactions were still taken into account as the major mechanism of the spin–lattice relaxation in bulk IL. However, contrary to previously reported data, both inter- and intramolecular contributions to the overall relaxation were taken into consideration in the present analysis. Thus, the total ^{1}H NMR spin–lattice relaxation rate, defined by the inverse of spin–lattice relaxation time, $R_1 \equiv 1/T_1$, measured in pure IL contains two contributions:

$$R_1^{BULK}(\omega) = R_{1,inter}(\omega) + R_{1,intra}(\omega), \tag{1}$$

where ω denotes the ^{1}H Larmor frequency ($\omega = 2\pi\nu = \gamma B_0$ is proportional to the proton gyromagnetic factor, γ, and magnetic field strength, B_0; ν is the linear resonance frequency). The first term in Eq. (1), $R_{1,inter}$, describes the intermolecular magnetic dipolar proton interactions modulated by the translational self-diffusion of molecules, whereas the second term, $R_{1,intra}$, expresses the intramolecular magnetic dipolar interactions among protons within the same molecule modulated by local molecular reorientations.

The relaxation mechanism caused by the translational self-diffusion has been analyzed on the basis of Torrey's model for viscous isotropic liquids and its contribution to the overall relaxation is given by [37]:

$$R_{1,inter} = C_{inter}\frac{n}{d^3\omega}\left[f(\delta, x) + f(\delta, \sqrt{2}x)\right], \tag{2}$$

where $C_{inter} = (3\pi/5)(\mu_0\gamma^2\hbar/(4\pi))^2$, n is the number of spins per unit volume, d is the distance of closest approach between molecules, and $\omega \propto 1/\tau_D$ where τ_D is the correlation time associated with the molecular jump displacements. $f(\delta, x)$ is an analytical function given in the original paper [37] where $\delta \equiv \langle r^2\rangle/(12d^2)$ with $\langle r^2\rangle$ being the mean square distance for the diffusion process, and $x \equiv (\omega d^2/D_b)^{1/2}$ where D_b denotes the self-diffusion constant.

The contribution of the local molecular reorientations to the total relaxation rate is given by the well-known Woessner's model that can be adopted for reorientations of an elongated [BMIm] cation around its long and short molecular axis, with characteristic correlation times τ_{rot}^L and τ_{rot}^S, respectively [38]:

$$R_{1,intra}(\omega) = C_{intra}[J_{intra}(\omega) + 4J_{intra}(2\omega)], \tag{3}$$

and

$$J_{intra}(\omega) = \frac{2}{15}\left[A_0\frac{2\tau_{c1}}{1+(\omega\tau_{c1})^2} + A_1\frac{2\tau_{c2}}{1+(\omega\tau_{c2})^2} + A_2\frac{2\tau_{c3}}{1+(\omega\tau_{c3})^2}\right], \tag{4}$$

where $C_{intra} = (9/8)(\mu_0\gamma^2\hbar/(4\pi))^2$, $\tau_{c1} = \tau_{rot}^S$, $1/\tau_{c2} = (1/\tau_{rot}^S) + (1/\tau_{rot}^L)$, $1/\tau_{c3} = (1/\tau_{rot}^S) + (4/\tau_{rot}^L)$ are the correlation times. $A_0 = (1 - 3\cos^2\alpha)^2/(4r^6)$, $A_1 = 3\sin^2\alpha/(4r^6)$, and $A_2 = 3\sin^4\alpha/(4r^6)$ are the geometric factors which depend on the intramolecular inter-proton distances, r, and orientations with respect to the molecular axis (α is the angle between the $\boldsymbol{r}$ vector and the symmetry axis of the molecule. The factors A_i ($i = 0, 1, 2$) can be estimated for an average conformation of the molecule [39].

The ^{1}H NMR spin–lattice relaxation rates, $R_1(\nu)$, obtained for neat IL in the frequency range from 10 kHz to 30 MHz with the use of FFC NMR relaxometry are presented in Fig. 2a as a function of the external magnetic field strength expressed in the

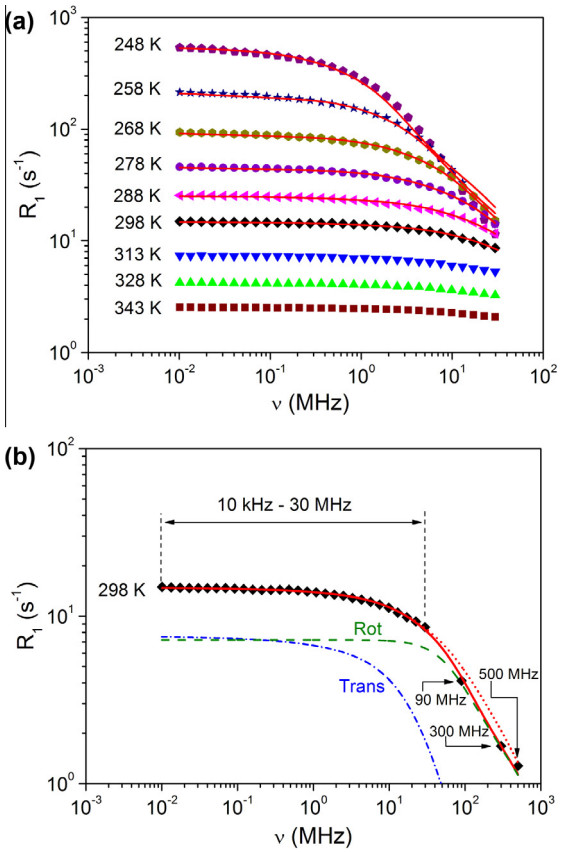

Fig. 2. (a) Frequency dependencies of the proton NMR spin–lattice relaxation rates for neat 1-butyl-3-methylimidazolium tetrafluoroborate ([BMIm][BF_4]) measured in the temperature range from 248 to 343 K. The solid lines are the best fits of Eq. (1) with Eqs. (2) and (3) to the experimental data; (b) The frequency dependency of the ^{1}H NMR spin–lattice relaxation rate in neat [BMIm][BF_4] measured at 298 K in the frequency range of 10 kHz–500 MHz; the solid line (in red) represents the best fit of Eq. (1) with Eqs. 2–4 with $r = 0.59$ (±0.03) nm (as a fitted parameter) and $n = 4.84 \times 10^{28}$ m^{-3}, $d = 0.5$ nm and $D_b = 1.38 \times 10^{-11}$ m^2/s (as fixed parameters) for the translational contribution (dash-dot line), and with $\tau^S_{rot} = 1.16$ (±0.03) $\times 10^{-9}$ s and $\tau^L_{rot} = 2.07$ (±0.04) $\times 10^{-10}$ s (as fitted parameters) and $A_0 = 5.78 \times 10^{57}$ m^{-6}, $A_1 = 6.91 \times 10^{57}$ m^{-6} and $A_2 = 1.09 \times 10^{58}$ m^{-6} (as fixed parameters evaluated for the structure of BMIm cation) for the rotational contribution (dash line). The dot line represents the fit computed for the FFC NMR experimental data from the frequency range of 10 kHz–30 MHz and simulated up to 500 MHz; the two fitted parameters were $\tau^S_{rot} = 1.01$ (±0.07) $\times 10^{-9}$ s and $\tau^L_{rot} = 3.43$ (±0.09) $\times 10^{-10}$ s, whereas the values of the other fixed parameters were taken as above. (For interpretation of the references to colour in this figure legend, the reader is referred to the web version of this article.)

frequency units. The amplitude of the relaxation rates decreases with increasing temperature and the curves exhibit an increasing dispersion with decreasing temperature. However, a visible frequency dependence above 1 MHz is clearly pronounced below room temperature. The relaxation data above room temperature showed almost linear dependence on frequency and thus they were not a subject of further analysis. Fig. 2b presents the spin–lattice relaxation data for bulk IL at 298 K obtained by FFC NMR relaxometry together with that measured with the use of permanent magnets operated at 90, 300, and 500 MHz. The values of the relaxation times at higher frequencies (i.e., above 30 MHz) were of great importance for data analysis because the shape of the dispersion curve allows for the better accuracy, especially for the determination of the intramolecular contribution [40]. Eq. (1) with Eqs. 2–4 was used to fit the theoretical models (both Torrey's and Woessner's one) to the experimental data in the extended frequency range (up to 500 MHz) as presented in Fig. 2b. To simplify the fitting procedure, some parameters were assessed: (a) the self-diffusion constant, D_b, was taken from literature [28], (b) the distance of closest approach, $d = 0.5$ nm, was estimated from the width of the elongated [BMIm] cation, (c) the number of spins per unit volume, $n = 4.84 \times 10^{28}$ m^{-3}, was calculated from the density of the IL under investigation, (d) the factors A_i were evaluated from the geometry of the [BMIm] cation: $A_0 = 5.58 \times 10^{57}$, $A_1 = 6.91 \times 10^{57}$, and $A_2 = 1.09 \times 10^{58}$ m^{-6}. Therefore, the correlation times τ^L_{rot} and τ^S_{rot} corresponding to the cation reorientation along its long and around its short axis, respectively, together with the distance r associated with the diffusion process were only the fitted parameters. The solid line in Fig. 2b represents the best fit to the experimental points. The dash-dot and dash lines show, respectively the translational and rotational contributions to the relaxation which are comparable especially in the low frequency range. The obtained values of the fitted parameters are: $r = 0.59$ nm, $\tau^S_{rot} = 1.16 \times 10^{-9}$ s and $\tau^L_{rot} = 2.07 \times 10^{-10}$ s. To check a validity of the fitting procedure in the frequency range cover only by FFC NMR relaxometry data, the experimental points were fitted in the range

of 10 kHz–30 MHz with fixed r parameter (r = 0.59 nm). The computed correlation times are then: $\tau_{rot}^{S} = 1.01 \times 10^{-9}$ s and $\tau_{rot}^{L} = 3.43 \times 10^{-10}$ s. As can be seen in Fig. 2b, the agreement between the result obtained for data fitted up to 500 MHz (solid line) and for data fitted only up to 30 MHz (dot line) are coincide well. Some discrepancies are observed only above 30 MHz. Therefore, for further analysis the r parameter was fixed and the relaxation data at 288, 278, 269, 258 and 248 K were fitted with simply two correlation times τ_{rot}^{L} and τ_{rot}^{S}; the self-diffusion constants, D_b, at particular temperature were taken from literature [28]. The solids lines in Fig. 2a represent the best fits to the experimental points. The obtained values of the rotational correlation times are shown in Fig. 3 together with the translational correlation times, τ_{trans}, calculated from the following relation: $\tau_{trans} = \langle r^2 \rangle / (6D_b)$.

The results presented indicate that both rotational and translational contributions to the overall relaxation are important and should be taken under consideration for neat ionic liquid under investigation.

3.2. ^{1}H NMR relaxation of IL in gel polymer electrolyte (GPE)

Fig. 4a presents the ^{1}H NMR spin–lattice relaxation R_1 dispersions profiles obtained for the gel polymer electrolyte at the same temperatures as for the neat IL. In contrast to the results collected in Fig. 2 (the pure IL), these dispersion curves show clearly visible frequency dependence, especially, in the low-frequency range, i.e., in kHz scale. For example, a direct comparison of the relaxation profiles obtained for the neat IL and GPE at 298 K is presented in Fig. 4b (open symbols – IL, full symbols – GPE). The observed low-frequency dispersion can be considered in terms of extremely long correlation times as that observed for the liquid molecules interacting with the pore walls in various porous media [41–44]. Additionally, as can be seen in Fig. 4a, an enhancement of the spin–lattice relaxation is also observed in the dispersion profiles in the frequency range of 1–10 MHz at the highest temperatures, i.e., at 313, 328 and 343 K. This effect could be explained as due to an effective segmental dynamics of the polymer matrix occurring close to and above the glass transition temperature (T_g = 325 K for pure acrylate polymer matrix) [31,45]. However, the electron paramagnetic resonance (EPR) signal detected in GPE (EPR spectra not shown) indicates that the observed enhancement of the spin–lattice relaxation observed in the dispersion profiles above 1 MHz at the highest temperatures is caused by unpaired electron spins of paramagnetic species interacting with nearby protons of IL cations. Such effect is called as a paramagnetic relaxation enhancement.

In contrast to the neat IL that can be considered as a bulk liquid with ions interacting with one another, the situation becomes more complicated when the IL ions are present in the GPE matrix. From the viewpoint of molecular dynamics, the ionic liquid confined in the GPE can be divided into two fractions: at (and/or close to) the polymer/IL interface and inside pools of IL in polymer matrix. The latter fraction of the IL is dominant and its ion molecules dynamically behave as "bulk-like". On the other hand, the fraction of the ions located at the interface are oriented with respect to the matrix "surface" via specific ion–polymer interactions. The correlation time of such molecules is significantly slow down but they still maintains translational mobility. However, the molecular dynamics of the ions in such a solid/liquid interface can exhibit significantly different character than in bulk IL. At the interface, the dynamics of the molecules is affected by the matrix surface topology. The rotational diffusion of the molecules executed about a preferential direction relative to the local surface is hindered and incomplete because of the surface. Consequently, this reorientation does not totally average out the intramolecular spin interactions and causes a fast drop of the correlation function only to some residual value. The intramolecular interaction is further modulated in time by translational displacement of the molecules along a rough and shaped pore surface with different local orientations. As a result of this displacement the adsorbed molecule changes its orientation according to the surface contour and to the external magnetic field B_o. Such molecular reorientations mediated by translational displacements of

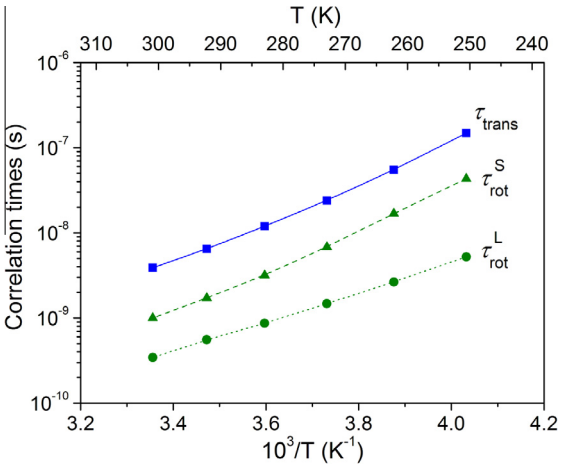

Fig. 3. Temperature dependencies of the fitted values of the rotational correlation time around long (circles) and short (triangles) axes of the cation in 1-butyl-3-methylimidazolium tetrafluoroborate together with the translational correlation times (squares) of the cation; the lines are given for eye guidance.

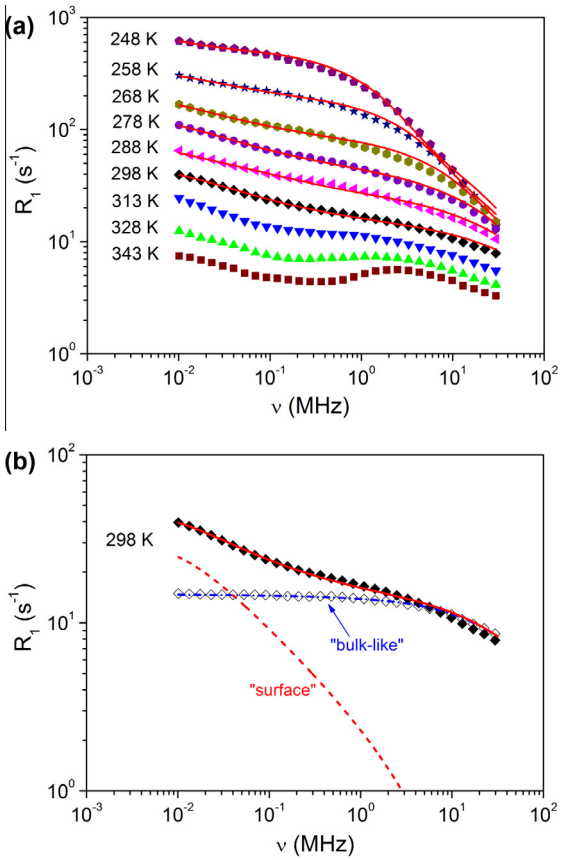

Fig. 4. (a) Frequency dependencies of the proton NMR spin–lattice relaxation rates in the gel polymer electrolyte (GPE) measured in the temperature range from 248 to 343 K; the solid lines are the best fits to the experimental data (see text); (b) The deconvolution of the overall relaxation into "*bulk-like*" and "*surface*" contributions in GPE at 298 K; open and full symbols denote the experimental data obtained for pure IL and GPE, respectively; the solid line (in red) represents the best fit of Eq. (8) with $A_{RMTD} = 1.9\ (\pm 0.6) \times 10^3\ s^{-3/2}$, $D_s = 3.3\ (\pm 0.4) \times 10^{-11}\ m^2/s$, $l_{min} = 1.1\ (\pm 0.4)$ nm, and $l_{max} = 37\ (\pm 5)$ nm (as fitted parameters) and $p = 0.5$ (as a fixed value – see text) for "surface" contribution (dash line), and fixed parameters for the "bulk-like" contribution (see Fig. 2b and text). (For interpretation of the references to colour in this figure legend, the reader is referred to the web version of this article.)

the molecules occur on a much slower time scale than bulk rotational or translational diffusion. This dynamical process known as *reorientation mediated by translational displacements* (RMTD) [46,47] is an efficient relaxation mechanism extending the orientation correlation times while maintaining the translational mobility. The RMTD becomes effective at low frequencies and was successfully applied to the interpretation of the relaxometry for liquids or liquid crystals confined to porous media, ionic liquids in polymer matrix, or molecules adsorbed on surfaces of macromolecules or particle aggregates [33,42,44,47–50]. In such systems the molecular translational diffusion despite the fact that it modulates intermolecular spin interactions, additionally modulates intramolecular proton spin interactions via the RMTD mechanism. RMTD requires polar surface and adsorbate molecules but without specific chemical bonding sites on the surfaces. The displacement of the molecules along the surface is executed by translational diffusion which can be the surface diffusion in the proper sense (weakly adsorbing system) or bulk mediated surface diffusion (BMSD) [51] (strongly adsorbing system). The RMTD process will be considered bellow as the dominating ^{1}H NMR spin–lattice relaxation mechanism of GPE in a low-frequency experimental regime.

As sketched in Fig. 5, for the IL/polymer system under investigation the RMTD process describes the molecular reorientation of IL cations determined by displacements between surface sites of different orientations. That is, the cation interacting with the polymer matrix, e.g., with its polar carbonyl group, adopts a preferential orientation relative to the local chain geometry. Translational displacements of the cation along the irregular polymeric wall will induce the *intra*molecular dipolar coupling fluctuations due to changes in the spin–spin vector orientation within the cation relative to the external magnetic field (see Fig. 5). In contrast to the bulk rotational diffusion, characterized by a relatively short correlation time, τ_{rot}, the RMTD correlation time, τ_{RMTD}, is up to 8 orders of magnitude longer and therefore these two dynamical processes can be considered independently [52–54].

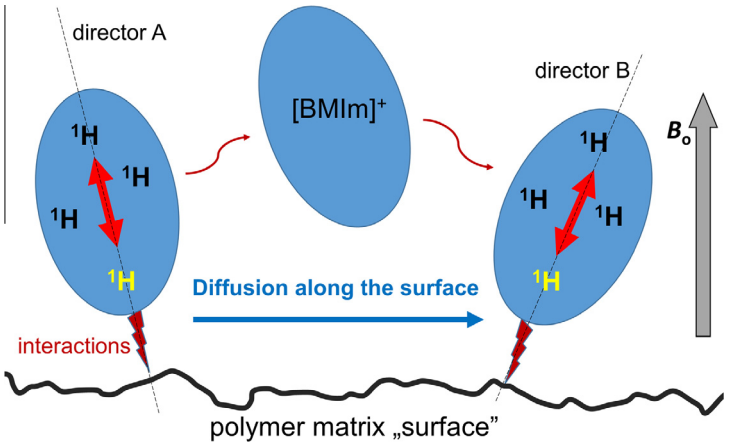

Fig. 5. Sketch presenting the reorientation of [BMIm] cations mediated by translational diffusion along the polymer/IL interface. $\boldsymbol{B_0}$ denotes external magnetic field direction.

The RMTD autocorrelation function, $G_{\mathrm{RMDT}}(t)$, whose decay reflects the molecular reorientation mediated by translational displacements, could be analyzed in terms of wave numbers, q, by analogy to the neutron scattering, and then in the whole wave number range [46]:

$$G_{\mathrm{RMTD}}(t) \propto \int_0^{\infty} S(q)p(q,t)dq, \tag{5}$$

and, for isotropic and quasi-two-dimensional space of the surface, $S(q)$ is the so-called *radial orientational structure factor* whereas $p(q,t)$ is the *q space propagator*. $S(q)$ factor can be related by a spatial Hankel transform to a *surface correlation function*, $g(r)$, that correlates the spatial orientation of the molecule at the sites on the surface separated by the distance r. On the other hand, the propagator $p(q,t)$ can be related to the probability density, $P(r,t)$, that the adsorbed molecule is displaced at a distance r along the surface in time t. That is, the geometrical and dynamical properties are independently expressed by the function $S(q)$ and the propagator $p(q,t)$, respectively. Assuming two-dimensional diffusion and the ordinary Gaussian probability density $P(s,t)$, one finds a simple exponential form of the propagator $p(q,t) = \exp(-t/\tau_q)$ [54], where $\tau_q = 1/(D_s q^2)$ is the characteristic time describing the exponential decay of the orientational correlation function for the diffusion mode with the wave number q, and D_s denotes the surface diffusion coefficient. On the other hand, the orientational structure factor $S(q)$ is a complex function of the wave numbers q (each diffusion mode might contribute with a different weight). However, the experimental power law frequency dispersion, $R_1^{\mathrm{RMTD}}(\omega) \propto \omega^{-\alpha}$, suggests the analytical form for the orientational structure factor in some cases: $S(q) = bq^{-\chi}$, where b is a constant and χ is the exponent varying in the range of 0–1 [33]. Taking into account the above mentioned assumptions, the spectral density function for the RMTD process adopts the form of the following integral over the wave numbers q in the limit from q_{min} to q_{max} [48]:

$$J_{\mathrm{RMTD}}(\omega) \propto \int_{q_{\mathrm{min}}}^{q_{\mathrm{max}}} q^{-\chi} \frac{2\tau_q}{1+(\omega\tau_q)^2} dq = \frac{2}{D_S} \int_{q_{\mathrm{min}}}^{q_{\mathrm{max}}} \frac{q^{2-\chi}}{q^4 + \left(\frac{\omega}{D_S}\right)^2} dq. \tag{6}$$

By substitution of z in place of $q(D_s/\omega)^{1/2}$ one can rewrite [48]:

$$J_{\mathrm{RMTD}}(\omega) \propto \omega^{-p} \int_{z_{\mathrm{min}}}^{z_{\mathrm{max}}} \frac{z^{3-2p}}{1+z^4} dz, \tag{7}$$

with $p = (1+\chi)/2$ ($p = 0.5$ for all modes equally weighted, i.e., $S(q) = \mathrm{const}$), $z_{\mathrm{min}} = (\omega_{c\ \mathrm{min}}/\omega)^{1/2}$, and $z_{\mathrm{max}} = (\omega_{c\ \mathrm{max}}/\omega)^{1/2}$, where $\omega_{c\ \mathrm{min}}$ and $\omega_{c\ \mathrm{max}}$ denote, respectively, the low and the high cutoff frequencies relating to the two-dimensional diffusion on the surface by the following relations: $\omega_{c\ \mathrm{min}}^{-1} = l_{\mathrm{max}}^2/4D_s$ and, $\omega_{c\ \mathrm{max}}^{-1} = l_{\mathrm{min}}^2/4D_s$, where l_{max} and l_{min} stand for the largest and smallest displacement distances on the pore wall, respectively.

The contribution of the RMTD process to the ^{1}H NMR spin–lattice relaxation can be expressed by the following equation [48,55]:

$$R_{1,\mathrm{intra}}^{\mathrm{RMTD}}(\omega) = A_{\mathrm{RMTD}} \left(\omega^{-p} \int_{z_{\mathrm{min}}}^{z_{\mathrm{max}}} \frac{z^{3-2p}}{1+z^4} dz + 4(2\omega)^{-p} \int_{z_{\mathrm{min}}/\sqrt{2}}^{z_{\mathrm{max}}/\sqrt{2}} \frac{z^{3-2p}}{1+z^4} dz \right), \tag{8}$$

where A_{RMTD} is the prefactor that depends on: (i) the residual ^{1}H–^{1}H dipolar coupling averaged by the local reorientations of the adsorbed molecule (i.e., restricted rotational diffusion or tumbling significantly faster than the RMTD process) that may occur around its preferential orientation on the surface, (ii) on the microstructural properties of the confined liquid, and (iii)

on the diffusion constant [49,50]. In the case of an equipartition of the diffusion modes with different wave numbers ($p = 0.5$), only four parameters (A_{RMTD}, D_s, l_{min}, and l_{max}) model the $R_{1,intra}^{RMTD}$ function.

The spin–lattice relaxation of liquids confined in porous media is usually evaluated assuming *two-phase fast-exchange model*. The exchange is characterized by an effective exchange time, τ_{exch}, which describes the exchange kinetics between two phases (fractions). The exchange is fast when referenced to the T_1 relaxation time scale but normally slow with reference to the RMTD process [50,56]. With the assumption that the RMTD process is much faster than the exchange process, the measured effective ^{1}H NMR spin–lattice relaxation rate in the gel polymer electrolyte (GPE) can by expressed by two contributions related to the "bulk-like" and "surface" fractions:

$$R_1^{SPE}(\omega) = R_1^{BULK}(\omega) + R_1^{SURF}(\omega). \quad (9)$$

The first term in the sum, R_1^{BULK}, corresponds to the contribution coming from the proton relaxation of the cations within pools of IL which behave like ions in the neat IL. Hence, R_1^{BULK} can be described by Eq. (1) after inserting Eqs. 2–4. The second contribution in the sum in Eq. (9), R_1^{SURF}, is related to the proton relaxation of the IL cations interacting with the polymer matrix at the polymer/IL interface. Their dynamics is affected by such interactions, and thus, the contribution R_1^{SURF} is expressed by Eq. (8).

The fits of the theoretical model descried by Eq. (9) to the all experimental data collected for GPE at particular temperatures are presented as solid lines in Fig. 4. The fits are quite satisfactory. The relaxation profiles obtained at the highest temperatures (i.e., at 313, 328 and 343 K) were not analyzed due to the observed paramagnetic relaxation enhancement. An exemplary deconvolution of the overall relaxation into "*bulk-like*" and "*surface*" contributions for the data obtained at 298 K is shown in Fig. 4b. The fitted parameters for the "surface" component are: $A_{RMTD} = 1.9 \times 10^3$ s$^{-3/2}$, $D_s = 3.3 \times 10^{-11}$ m^2/s, $l_{min} = 1.1$ nm, and $l_{max} = 37$ nm, with fixed $p = 0.5$ characteristic for an equipartition of the diffusion modes with different wave numbers. The parameters of the bulk IL contribution were fixed to those obtained from the fitting procedure applied for neat IL at particular temperature. The longest correlation time $\tau_{RMTD\ max}$ related to the RMTD process evaluated from $2\pi l_{max}^2/4D_s$ is of the order of 10^{-5} s. It should be noted that the low-frequency plateau of the dispersion profile, thus also the low frequency cut-off, is not accessible to our FFC NMR experiment and therefore, the l_{max} distance obtained from the fitting procedure is just an approximation, similarly as the frequency ($\omega_{c\ min}^{-1} = l_{max}^2/4D_s$) which in fact is well below the lowest frequency accessible to the experiment. As presented in Fig. 4b, the R_1^{SURF} contribution to the overall relaxation is dominant in the lowest frequency range.

Fig. 6 presents the self-diffusion coefficients, D_s ("surface") and D_b ("bulk-like"), obtained from fitting procedure of the relaxation dispersion data of IL cations confined in the structure of GPE. The results obtained indicate that the fraction of the cations located at (and/or close to) the polymer/IL interface is characterized by unique translational mobility reflected by the self-diffusion constants higher than those found for the cations in the bulk. This extraordinary finding is in agreement with the increased ionic conductivity observed in this IL-polymer electrolyte in comparison to that of bulk IL. The question arises, how to explain such a significantly higher self-diffusion constants of the cations at the polymer/IL interface?

3.3. Ion conducting pathways

Before trying to answer the above question, let's analyze some examples of unexpectedly high self-diffusion coefficients or ionic conductivity in solid electrolytes. As shown for Nafion® membranes modified with [BMIm]$^+$ cation (by the ion

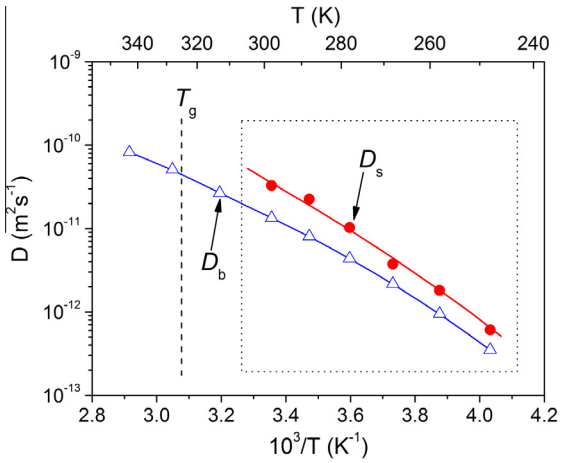

Fig. 6. Temperature dependencies of the self-diffusion coefficients obtained for the [BMIm] cations in gel polymer electrolyte. The diffusion constants of cations diffusing along the polymer/IL interface (D_s, "surface") and in the pools of IL in the polymer matrix (D_b, "bulk-like" [28]) are represented by full circles and open triangles, respectively; the lines are given for eye guidance. $T_g = 325$ K for pure acrylate polymer matrix (see text).

exchange), the self-diffusion constant of the electrolyte molecules (IL + water) close to the channel and cluster walls was somewhat higher than that measured for the neat [BMIm][BF_4] [55]. Although initially the authors tried to relate this effect to different hydration conditions of the cation molecules in the pure IL and Nafion/[BMIm]$^+$ modified membrane, in the subsequent studies they rejected this hypothesis showing that there is no influence of water content on the spin–lattice dispersion observed for two IL samples of different moisture content [49]. Another reported example concerns the polymeric gel electrolyte composed of [BMIm][BF4] and poly(vinylidenefluoride-cohexafluoropropylene) (PVdF–HFP) polymer [57]. It was found that the values of the ionic conductivity of the IL polymer membranes with 80 and 90 wt% of IL were higher than that of pure IL. The *polymer chain breathing model* has been suggested to explain this effect assuming that ion pairs with compensated electrical charge normally present in liquid electrolyte are broken in the presence of polymer chains. This reasonable explanation was supported by studies of other ion-conducting gel electrolytes [58–60].

In the present study the ionic liquid is mostly entrapped during the photopolymerization process in the pools of the gel matrix. They are large enough to not alter the motion of ionic liquid and it behaves like the bulk liquid. Therefore, the polymer matrix plays a minor role on the dynamics of bulk-like fraction of confined IL. The situation becomes different for the fraction of ionic liquid aggregates close to polymer/IL interface. They are interacting with the "surface" of polymer matrix as revealed by the low-frequency dispersion of the proton spin–lattice relaxation time of the IL confined in the GPE (Fig. 4) measured by the FFC NMR relaxometry method. The presence of the specific interaction of the gel matrix with either cations (and/or anions) decreases the tendency to form ion-pairs or aggregates, resulting in an increase in the total number of ion carriers in the polymer gel electrolytes [24,59]. Additionally, the interaction leads to a decrease in the size of ion complexes which can explain the higher D_s values of the cations at the polymer/IL interface than those of the D_b of cations in the bulk-like fraction of IL. The both effects: the increase in the total number of ion carriers and the decrease in the size of ion complexes can account for the increase in the ionic conductivity in GPE.

In terms of specific interactions between polymer chain and IL ions we suggest the existence of a characteristic *interphase* which separates the solid polymer and bulk-like ionic liquid phases. Within this interphase specific layers of ordered ions may be created that can play a role of pseudo two-dimensional channels through which some new ion conducting pathways may be created in the nanometric scale, significantly different than in the bulk IL.

4. Conclusions

The results presented in this paper have shown that ionic liquid molecules are characterized by different dynamic properties within the pools of IL in the gel polymer matrix and at the polymer/IL interface. Applying the nuclear magnetic resonance relaxometry method and proper theoretical models, i.e. *Torrey's model* for translational self-diffusion and *Woessner's one* for reorientations around a long and a short molecular axis of the [BMIm] cation, and *reorientation mediated by translational displacements* for analysis of the surface diffusion, we were able to distinguish the translational dynamics of the IL cations within the pores of GPE and of the cations interacting with the polymer matrix at the polymer/IL interface. It was shown that the self-diffusion of cations migrating at the solid/liquid interface is characterized by the diffusion constants which are higher than in pure IL. However, we should keep in mind that these both diffusion coefficients are referred to different time and length scale. Apart from this finding, the ionic conductivity measured for GPE by impedance method was found to be twice higher than that of pure IL. On the basis of these experimental facts, we speculate the existence of an *interphase* which is formed between the polymer matrix and the pools of IL in the matrix. The conductivity increase is proposed to be explained by the interaction of ionic liquid aggregates at polymer/IL interface. It seems that such interaction fascinatingly aids to the increase in the total carrier number in the polymer gel electrolyte and leads to the enhancement of the electrical conductivity. This interaction prohibits the formation of ion clusters or associates and decreases the size of ion complexes in the interphase. In this phase ions may create new ionic-conducting pathways which can play an important role in ionic conduction observed at the microscopic level. Due to specific properties of IL ions interacting with the active polymer matrix groups in such interphase, an effective diffusion mechanism involving highly dissociated ions coming from this interphase should be considered. This working hypothesis must be supported by further systematic investigation, which is now in progress.

Acknowledgements

This work was partially supported by the Research Project of Poznan University of Technology 03/32/DSPB/0504. The authors also thank Dr. W. Bednarski from Institute of Molecular Physics Polish Academy of Sciences for help in EPR measurements.

References

[1] M.A. Lauffer, Motion in Biological Systems, Alan R. Liss, New York, 1989.
[2] W.S. Price, NMR Studies of Translational Motions. Principles and Applications, Cambridge University Press, New York, 2009.
[3] B. Geil, O. Isfort, B. Boddenberg, D.E. Favre, B.F. Chmelka, F. Fujara, J. Chem. Phys. 116 (2002) 2184–2193.
[4] R. Meier, D. Kruk, E.A. Rössler, Chem. Phys. Chem. 14 (2013) 3071–3081.
[5] P.G. Bruce, Solid State Electrochemistry, Cambridge University Press, 1995.
[6] H. Ohno, Electrochemical Aspects of Ionic Liquids, John Willey & Sons, Hoboken: New Jersey, 2011.
[7] K.S. Han, S. Li, E.W. Hagaman, G.A. Baker, P. Cummings, S. Dai, J. Phys. Chem. C 116 (2012) 20779–20786.

[8] H. Sakaebe, H. Matsumoto, Electrochem. Commun. 5 (2003) 594–598.
[9] H. Nakagawa, S. Izuchi, K. Kuwana, T. Nukuda, Y. Aihara, J. Electrochem. Soc. 150 (2003) A695–A700.
[10] C. Nanjundiah, S.F. McDevitt, V.R. Koch, J. Electrochem. Soc. 144 (1997) 3392–3397.
[11] M. Ue, M. Takeda, A. Toriumi, A. Kominato, R. Hagiwara, Y. Ito, J. Electrochem. Soc. 150 (2003) A499–A502.
[12] M. Doyle, S.K. Choi, G. Proulx, J. Electrochem. Soc. 147 (2000) 34–37.
[13] M.d.A.B.H. Susan, A. Noda, H. Mitsushima, M. Watanabe, Chem. Commun. (2003) 938–939.
[14] P. Wang, S.M. Zakeeruddin, I. Exnar, M. Gratzel, Chem. Commun. (2002) 2972–2973.
[15] P. Wang, S.M. Zakeeruddin, P. Comte, I. Exnar, M. Gratzel, J. Am. Chem. Soc. 125 (2003) 1166–1167.
[16] M. Morita, T. Shirai, N. Yoshimoto, M. Ishikawa, J. Power Sources 139 (2005) 351–355.
[17] M.-H. Ryou, Y.M. Lee, K.Y. Cho, G.-B. Han, J.-N. Lee, D.J. Lee, J.W. Choi, J.-K. Park, Electrochim. Acta 60 (2012) 23–30.
[18] I. Stępniak, E. Andrzejewska, A. Dembna, M. Galinski, Electrochim. Acta 121 (27–3) (2014) 3.
[19] K. Matsumoto, S. Sogabe, T. Endo, J. Polym. Sci., Part A: Polym. Chem. 50 (2012) 1317–1324.
[20] C. Gerbaldi, J.R. Nair, S. Ferrari, A. Chiappone, G. Meligrana, S. Zanarini, P. Mustarelli, N. Penazzi, R. Bongiovanni, J. Membr. Sci. 423 (2012) 459–467.
[21] E. Andrzejewska, I. Stępniak, Polimery/Polym. [Warsaw] 51 (2006) 859–861.
[22] I. Stępniak, E. Andrzejewska, Electrochim. Acta 54 (2009) 5660–5665.
[23] A. Magistris, E. Quartarone, P. Mustarelli, Y. Saito, H. Kataoka, Solid State Ionics 152 (2002) 347–354.
[24] E. Andrzejewska, A. Dembna, A. Rachocki, J. Tritt-Goc, Ionic liquids polymer electrolytes prepared by in situ photopolymerization, in: 3rd European Symposium of Photopolymer Science, Vienna, September 9th–12th, Proceedings, 2014, p. IL-2.
[25] K. Ueno, H. Tokuda, M. Watanabe, Phys. Chem. Chem. Phys. 12 (2010) 1649–1658.
[26] A.O. Seyedlar, S. Stapf, C. Mattea, Phys. Chem. Chem. Phys. 17 (2015) 1653–1659.
[27] D. Kruk, R. Meier, A. Rachocki, A. Korpała, R.K. Singh, E.A. Rössler, J. Chem. Phys. 140 (2014) 244509.
[28] D. Nama, P.G. Anil Kumar, P.S. Pregosin, T.J. Geldbach, P.J. Dyson, Inorg. Chim. Acta 359 (2006) 1907–1911.
[29] E.D. Hazelbaker, S. Budhathoki, A. Katihar, J.K. Shah, E.J. Maginn, S. Vasenkov, J. Phys. Chem. B 116 (2012) 9141–9151.
[30] I. Changa, F. Fujara, B. Geilb, G. Hinzea, H. Sillescua, A. Töllea, J. Non-Cryst. Solids 172–174 (2004) 674–681.
[31] D. Kruk, A. Herrmann, E.A. Rössler, Prog. Nucl. Magn. Reson. Spectrosc. 63 (2012) 33–64.
[32] A. Rachocki, J. Tritt-Goc, Food Chem. 152 (2014) 94–99.
[33] R. Kimmich, E. Anorado, Progr. Nucl. Magn. Reson. 44 (2004) 257–320.
[34] A. Dembna, Doctoral Thesis, Poznan University of Technology, 2013.
[35] Avogadro Software, <http://avogadro.cc>.
[36] A. Abragam, The Principles of Nuclear Magnetism, Oxford University Press, Oxford, 1961.
[37] H.C. Torrey, Phys. Rev. 92 (1953) 962–969.
[38] D.E. Woessner, J. Chem. Phys. 36 (1962) 1–4.
[39] A. Gradišek, P.J. Sebastião, S.N. Fernandes, T. Apih, M.H. Godinho, J. Seliger, J. Phys. Chem. B 16 (2014) 5600–5607.
[40] K. Hayamizu, S. Tsuzuki, S. Seki, Y. Umebayashi, J. Phys. Chem. B 116 (2012) 11284–11291.
[41] R. Kimmich, W. Nusser, T. Gneiting, Colloids Struct. 45 (1990) 283–302.
[42] R. Kimmich, H.W. Weber, Phys. Rev. B 47 (1993) 11788–11794.
[43] F. Barberon, J.-P. Korb, D. Petit, V. Morin, E. Bermejo, Phys. Rev. Lett. 90 (2003) 116103.
[44] J. Tritt-Goc, A. Rachocki, M. Bielejewski, Soft Matter 10 (2014) 7810–7818.
[45] A. Rachocki, J. Kowalczuk, J. Tritt-Goc, Solid State Nucl. Magn. Reson. 30 (2006) 192–197.
[46] T. Zavada, R. Kimmich, J. Chem. Phys. 109 (1998) 6839–6929.
[47] R. Kimmich, NMR Tomography, Diffusometry, Relaxometry, Springer, Berlin, 1997.
[48] M. Vilfan, T. Apih, P.J. Sebastião, G. Lahajnar, S. Žumer, Phys. Rev. E 76 (2007) 051708.
[49] C.F. Martins, L. Neves, I.M. Coelhoso, F. VacaChávez, J.G. Crespo1, P.J. Sebastião, Fuel Cells 13 (2013) 1166–1176.
[50] P.J. Sebastião, D. Sousa, A.C. Ribeiro, M. Vilfan, G. Lahajnar, J. Seliger, S. Žumer, Phys. Rev. E 72 (2005) 061702.
[51] O.V. Bychuk, B. O'Shaughnessy, J. Phys. II 4 (1994) 1135.
[52] R. Kimmich, S. Stapf, P. Callaghan, A. Coy, Magn. Reson. Imaging 12 (1994) 339–343.
[53] S. Stapf, R. Kimmich, J. Niess, J. Appl. Phys. 75 (1994) 529–537.
[54] R. Kimmich, S. Stapf, R.-O. Seitter, P. Callaghan, E. Khozina, Mater. Res. Soc. Symp. Proc. 366 (1995) l89–200.
[55] L.A. Neves, P.J. Sebastião, I.M. Coelhoso, J.G. Crespo, J. Phys. Chem. B 115 (2011) 8713–8723.
[56] E. Anorado, F. Grinberg, M. Vilfan, R. Kimmich, Chem. Phys. 297 (2004) 99–110.
[57] S.K. Chaurasia Shalu, R.K. Singh, S. Chandra, J. Phys. Chem. B 117 (2013) 897–906.
[58] J. Kowalczuk, M. Bielejewski, A. Łapiński, R. Luboradzki, J. Phys. Chem. B 118 (2014) 4005–4015.
[59] M.d.A.B.H. Susan, T. Kaneko, A. Noda, M. Watanabe, J. Am. Chem. Soc. 127 (2005) 4976–4983.
[60] M. Bielejewski, A. Puszkarska, J. Tritt-Goc, Electrochim. Acta 165 (2015) 122–129.